NANO LETTERS

2008
Vol. 8, No. 5
1439-1445

Quantum Dot−Fluorescent Protein Pairs as Novel Fluorescence Resonance Energy Transfer Probes

Allison M. Dennis and Gang Bao*

Department of Biomedical Engineering, Georgia Institute of Technology and Emory University, 313 Ferst Drive, Atlanta, Georgia 30332

Received February 5, 2008; Revised Manuscript Received March 21, 2008

ABSTRACT

Fluorescence resonance energy transfer (FRET) characteristics, including the efficiency, donor−acceptor distance, and binding strength of six fluorescent protein (FP)−quantum dot (QD) pairs were quantified, demonstrating that FPs are efficient acceptors for QD donors with up to 90% quenching of QD fluorescence and that polyhistidine coordination to QD core−shell surface is a straightforward and effective means of conjugating proteins to commercially available QDs. This provides a novel approach to developing QD-based FRET probes for biomedical applications.

Semiconductor quantum dots (QDs) are exceptionally bright fluorescent nanoparticles that have garnered much attention recently as an emerging tool for biomedical applications. In the decade since QDs were first rendered water soluble,[1,2] thereby making them relevant for biological studies, they have been applied to cell tracking studies,[3,4] cancer imaging,[5,6] and flow cytometry[7] and used to label membrane proteins.[8,9] The potential applications for QDs also extend to fluorescence-based detection of enzymatic activities, particularly when QDs are utilized as either a donor or an acceptor for fluorescence (or Förster) resonance energy transfer (FRET).[10–14] QDs make excellent FRET donors because of their exceptional brightness and high quantum yields,[15–17] their capacity to bind multiple acceptor molecules,[18] and the unique qualities of their characteristic excitation and emission spectra.[16] The broad excitation range of the QDs allows them to be excited far from the excitation range of the acceptor molecule, minimizing the background due to direct excitation of the acceptor, while the narrow and tunable QD emission peak can be optimally matched with the absorption spectrum of the desired acceptor. In addition, all different-sized QDs that emit in the visible range are best excited by UV light, allowing for color multiplexing.[19] Recent reports have described the approaches using QDs as a FRET donor with organic fluorophores, organic quenchers, or gold nanoparticles as the acceptor.[10–12]

There are, however, several areas where the QD-based FRET approach could be improved. Currently, when commercially available QDs are used as donors for FRET studies, the FRET acceptor is either covalently bound to the organic coating using standard cross-linking chemistry[10] or bound using a biotin−streptavidin interaction.[11] The bioconjugation involved typically requires multiple steps and tedious purification and may cause nanoparticle aggregation. In addition, linking the FRET pair via the organic coating on the QD can substantially increase the distance between the acceptor and the center of the QD. Because the FRET efficiency is inversely proportional to the distance between the donor and acceptor molecules to the sixth power,[20] the increased separation due to the bulky water-soluble organic coating can significantly reduce the energy transfer efficiency. The biotin−streptavidin interaction is a technically simpler conjugation strategy but results in large probe size and further increases the distance between the donor and acceptor molecules, thereby substantially reducing the FRET efficiency. As an alternative, polyhistidine peptide tags that utilize noncovalent, high affinity binding to metals have been developed and thoroughly characterized.[12,18,21,22] Since polyhistidine is able to chelate ions accessible in the ZnS capping layer of the most commonly used CdSe/ZnS core−shell QDs,[22] the use of polyhistidine peptide tags in a QD-based FRET assay results in a much smaller distance between the donor and acceptor compared with other acceptor bioconjugation schemes. However, to date this strategy has been demonstrated for protein−QD conjugation only with QDs water-solubilized with a dihydrolipoic acid (DHLA) coating, which are not commercially available and tend to aggregate under acidic conditions.[23] The polyhistidine peptide tag has been used with commercially available QDs (QDots from

* Corresponding author. Tel: 1-404-385-0373. Fax: 1-404-894-4243. E-mail: gang.bao@bme.gatech.edu.

10.1021/nl080358+ CCC: $40.75
Published on Web 04/16/2008

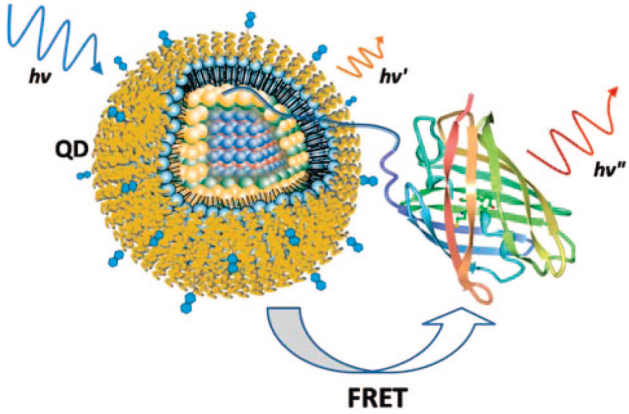

Figure 1. Schematic diagram of the FRET interaction between a quantum dot, specifically a T2-MP EviTag (Evident Technologies) and a GFP-like fluorescent protein. A polyhistidine sequence inserted at the N-terminus of the mCherry shown here coordinates to the ZnS capping layer of the QD, bringing the two into close proximity. Under excitation of the QD, energy is nonradiatively transferred to the fluorescent protein and sensitized emission is observed. (EviTag image courtesy of Evident Technologies. mCherry produced with PDB Protein Workshop 1.50 using the PDB 2H5Q).

Invitrogen) to demonstrate the utility of QDs as a bioluminescence resonance energy transfer (BRET) acceptor with luciferase as the donor;[13] however in this case the histidine tag interacted with Ni^{2+} ions chelated by a high density of carboxyl groups in the organic coating, rather than binding directly to the inorganic QD surface. While this approach maintained some of the benefits of the his-tag (such as the ease in incorporating the tag into a recombinant protein and the minimal steps necessary for bioconjugation), the distance between the donor and acceptor is increased due to the organic coating on the QD, thus eliminating one of the key benefits of using the his-tag self-assembly strategy to bind biomolecules to QDs to form FRET-based probes.

Herein we report the development of fluorescent protein−QD based FRET probes using polyhistidine coordination to the inorganic surface of commercially available QDs, demonstrating that fluorescent proteins (FPs) are exceptional FRET acceptors for QD donors. The use of fluorescent proteins as acceptors has several benefits. For example, standard molecular biology techniques can easily be used to modify the FPs to include the polyhistidine tag, a variety of linkers between the protein bulk and the tag, and amino acid sequences that could contribute to the functionality of the QD-FRET probe, such as a cleavage sequence for a protease to produce a FRET-based probe to measure enzyme activity. Once a plasmid for the recombinant protein is designed, fluorescent proteins can be expressed in *E.coli* in large quantities, and the presence of the polyhistidine on his-tagged proteins facilitates protein purification using immobilized metal affinity chromatography (IMAC). The large variety of GFP-like fluorescent proteins now available with emission wavelengths spanning the entire visible range[24,25] also provides an array of possible fluorescent protein acceptors for QDs with different colors.

The schematic in Figure 1 demonstrates how the interaction between a his-tagged fluorescent protein[26] and a T2-

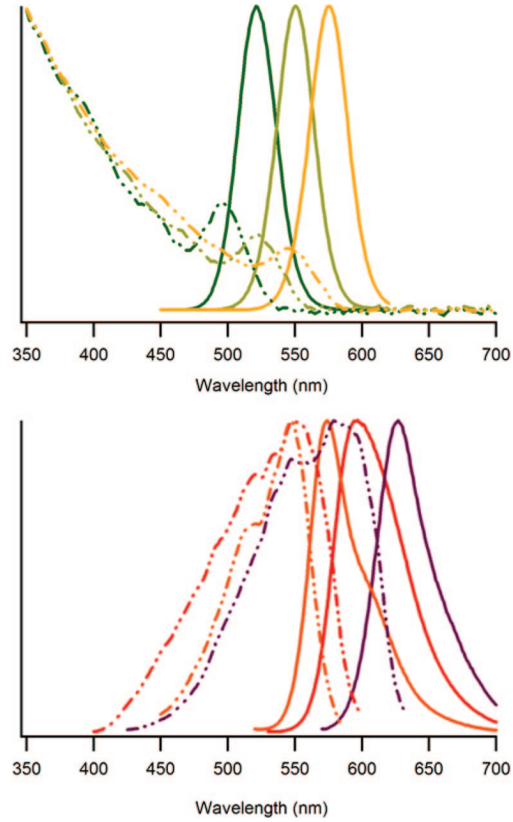

Figure 2. Top: Absorbance (dashed lines) and emission spectra (solid lines, with emission peaks from left to right) of 520, 540, and 560 nm T2-MP Carboxyl EviTag QDs. Bottom: Excitation (dashed lines) and emission spectra (solid lines, with emission peaks from left to right) of fluorescence proteins mOrange, tdTomato, and mCherry.

MP EviTag (Evident Technologies, Troy, NY) results in FRET. The carboxyl-functionalized T2-MP EviTag is a CdSe/ZnS core−shell QD, coated with lipid−PEG manufactured by Avanti for water solubility. The fluidity of this micellular lipid−PEG coating is likely what enables the polyhistidine to interact directly with the core−shell QD surface. The polyhistidine sequence was inserted at the N-terminus of the protein structure followed by three glycines that act as a flexible linker between the polyhistidine sequence and the barrel structure of the GFP-like fluorescent protein. Three different-colored T2-MP carboxyl-functionalized EviTags, QD520, QD540, and QD560, named for their peak emission wavelengths of 520, 540, and 560 nm (all ±10 nm), respectively, were combined with three fluorescent proteins from the mFruit family: mCherry and mOrange are both monomeric, while tdTomato is a tandem dimer. The spectra for all of the donors and acceptors can be found in Figure 2, while a list of other QD and FP characteristics can be found in Table 1.

Standard molecular biology techniques were used to produce the fluorescent proteins necessary for this study. Plasmids containing the mOrange, tdTomato, and mCherry coding regions were generously provided by Roger Tsien's laboratory at UCSD. These plasmids were altered using PCR mutagenesis to remove any unnecessary amino acids from the expressed region, producing a negative control lacking

Table 1. FRET Donor and Acceptor Specifications

FRET acceptor: fluorescent protein[a]						
acceptor	peak excitation (nm)	peak emission (nm)	extinction coefficient (M^{-1} cm^{-1})	quantum yield	time to photobleach ($t_{0.5}$, min)	molecular weight (kDa)
mOrange	548	562	71000	0.69	6.4	27
tdTomato	554	581	138000	0.69	70	54
mCherry	587	610	72000	0.22	68	27

FRET donor: T2-MP carboxyl EviTags[b]						
donor	water-soluble coating	preferred excitation (nm)	emission peak (nm)	quantum yield	core−shell diameter (nm)	hydrodynamic diameter (nm)
QD520	lipid PEG with		520±10	0.28	7.5	
QD540	carboxyl	≤400	540±10	0.35	7.7	∼25
QD560	terminal groups		560±10	0.31	8.0	

[a] Fluorescent protein specifications previously published.[24] [b] EviTag specifications published at www.evidenttech.com or provided by Evident Technologies technical support.

Table 2. Donor−Acceptor Pair Results Summary

donor−acceptor pair	J (10^{-15} M^{-1} cm^3)	R_0 (Å)	R (Å)	E at 1:1 QD:FP[a]	max E	K_D (nM)
QD520-mOrange	3.744	47.81	57.4 ± 6.6	0.261	0.761	92.7 ± 9.6
QD520-tdTomato	8.523	54.84	53.8 ± 3.4	0.428	0.867	61.2 ± 6.6
QD540-tdTomato	11.259	58.49	52.7 ± 3.9	0.504	0.902	43.2 ± 1.3
QD520-mCherry	3.339	46.91	52.0 ± 4.3	0.302	0.713	72.0 ± 6.7
QD540-mCherry	5.595	52.06	56.2 ± 4.5	0.343	0.798	69.7 ± 3.0
QD560-mCherry	7.303	52.56	53.6 ± 5.1	0.401	0.838	59.8 ± 2.9

[a] Pairs that did not have 1:1 QD:FP data points were given values based on the relative QD emission curve fits.

a polyhistidine sequence. In a separate plasmid, nucleic acids were inserted to add six histidines and three glycines to produce the his-tag and linker. Proteins were expressed from these modified plasmids in the Rosetta 2(DE3) strain of *E. coli* and purified using chromatographic methods. The his-tagged proteins could be isolated readily using IMAC, but the control proteins had to be purified using a hydrophobic column followed by size-exclusion chromatography. Details of the plasmid mutagenesis and protein expression and purification can be found in the Supporting Information. The plasmids were sequenced to verify the modifications, and the protein purity was confirmed using SDS-PAGE.

To select QD-FP pairs for FRET assays, Igor (v.5.05A, WaveMetrics, Inc., Lake Osweego, OR) was used as previously described[27] to calculate the overlap integral and Förster distance for each of the FRET pairs (Table 2). The spectral overlap integral

$$J = \int F_D(\lambda)\varepsilon_A(\lambda)\lambda^4 \, d\lambda \quad (1)$$

describes the degree of coincidence between the donor emission and the acceptor absorption, where F_D is the emission spectrum of the donor, ϵ_A is the molar extinction coefficient of the acceptor, and λ is the wavelength in nanometers. Once the overlap integral was calculated, the Förster distance, R_0, or the distance between the donor and acceptor at which the FRET efficiency is 50%, was determined using the equation

$$R_0^6 = (8.785 \times 10^{-5})\kappa^2 Q_D \frac{J}{n_r^4} \quad (2)$$

where κ^2 is the dipole orientation factor, assumed to be 2/3, Q_D is the quantum yield of the donor, and n_r is the refractive index of the medium. Based on the results of these calculations and an examination of the QD and FP spectra, six FRET pairs were chosen for evaluation, as shown in Table 2. The other three possible FRET pairs (QD540-mOrange, QD560-mOrange, and QD560-tdTomato) were excluded due to the significant overlap in the emission spectra of the QDs and FPs, which would hinder accurate deconvolution of the emission peaks and the analysis of the FRET assays.

Assays examining the FRET efficiency of the various pairs were carried out in black, flat-bottomed, nonbinding 384-well plates. Alternating serial dilutions of fluorescent proteins were made to produce a range of average QD:FP ratios ranging from 16 FPs per QD to fewer than 0.2 FPs per QD. EviTag QDs were then added to the wells at a final concentration of 50 nM. All of the assays were prepared in PBS, pH 7.4, with 1% bovine serum albumin (BSA) added to minimize any nonspecific binding. After 15 min of conjugation, the emission spectra were measured in a Tecan Safire multiplate reader with an excitation wavelength of 400 nm, excitation bandwidth of 12 nm, emission bandwidth of 5 nm, and a step size of 3 nm. All of the assays were performed in triplicate, as were FP-only controls. As shown in Figures 3 and 4, all three of the his-tagged fluorescent proteins exhibited an ability to substantially quench the QD emission due to FRET, as demonstrated by the across-the-board decrease in the QD emission peak, the correlation between the spectral overlap of the donor−acceptor pair, and the quenching efficiency (Table 2). Sensitized emission was observed from each of the protein acceptors, although tdTomato and mOrange (Figure 3) emitted more strongly than mCherry (Figure 4). The assays were each repeated using unmodified fluorescent proteins without the his-tag as negative controls to ensure that the QD/FP binding was indeed mediated by the polyhistidine, and a second control utilized a short His10 peptide without a fluorophore (Anaspec, San Jose, CA) to demonstrate that the binding of the polyhistidine to the core−shell surface was not causing

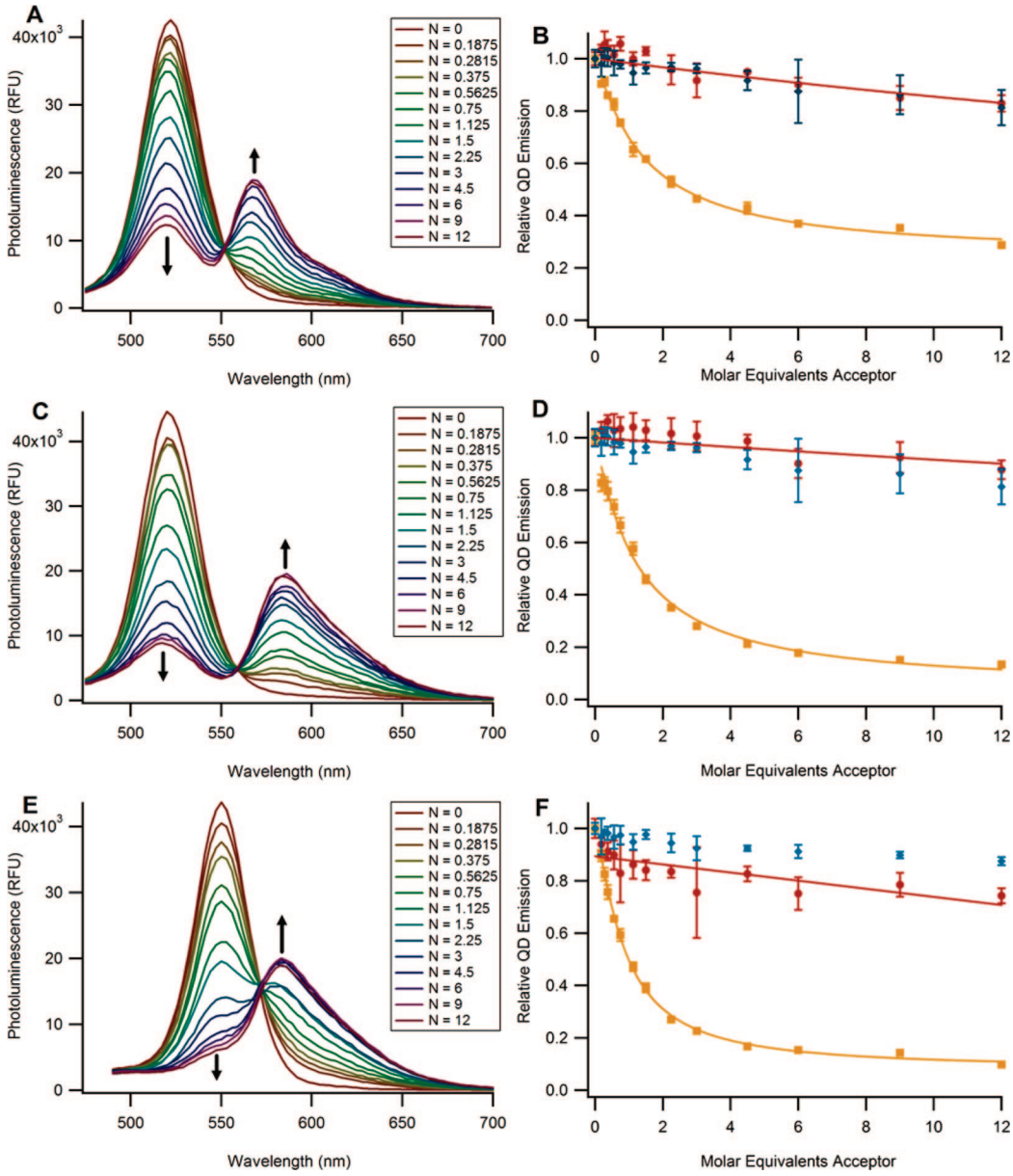

Figure 3. FRET results using fluorescent proteins mOrange and tdTomato as acceptors and a QD donor. (A, C, and E) Spectra of QD520 + His6-mOrange, QD520 + His6-tdTomato, and QD540 + His6-tdTomato, respectively. *N* is the average number of fluorescent proteins per QD. (B, D, and F) Relative area under the QD emission peak of background-subtracted spectra. The non-his-tagged FP control is represented as a circle (●), the His10-only (no fluorescent protein) control is a diamond (♦), and the His6-FP is represented by a square (■). Data are represented as a mean ± standard deviation of $n = 3$.

contact-quenching of the QD or otherwise affecting the QD emission.

Although the direct excitation of the FPs was minimal (see Figure S1 in the Supporting Information), the background emission was subtracted from each of the FRET spectra at the same FP concentration at the beginning of the analysis. Each background-subtracted spectrum was then deconvolved using PeakFit (v.4.12, Systat, San Jose, CA); the symmetrical EviTag emission was fitted to a Voigt area peak, while an exponentially modified Gaussian (EMG) curve was used to account for the tailing seen in the asymmetrical FP emission. The areas under the QD peaks with FRET were normalized by the area under the QD spectrum in the absence of FP. The resulting normalized QD emission intensities were plotted versus the acceptor concentrations in Figures 3 and 4. The non-his-tagged FP results were fitted to the Stern−Volmer equation (see Supporting Information). To estimate the strength of binding between the EviTags and the his-tagged proteins under steady-state conditions, the His6-FP data shown in Figures 3 and 4 were fitted to a modified Hill equation[28]

$$\frac{F_{DA}}{F_D} = 1 - E_{max}\left[\frac{1}{1 + (K_D/c)^h}\right] \quad (3)$$

where F_{DA} is the fluorescence of the donor in the presence of the acceptor, F_D is the fluorescence of the donor in the absence of the acceptor, E_{max} is the maximum FRET efficiency, c is the concentration of the acceptor, h is the Hill coefficient, and K_D is a nominal dissociation constant defined as the acceptor concentration at which there is 50%

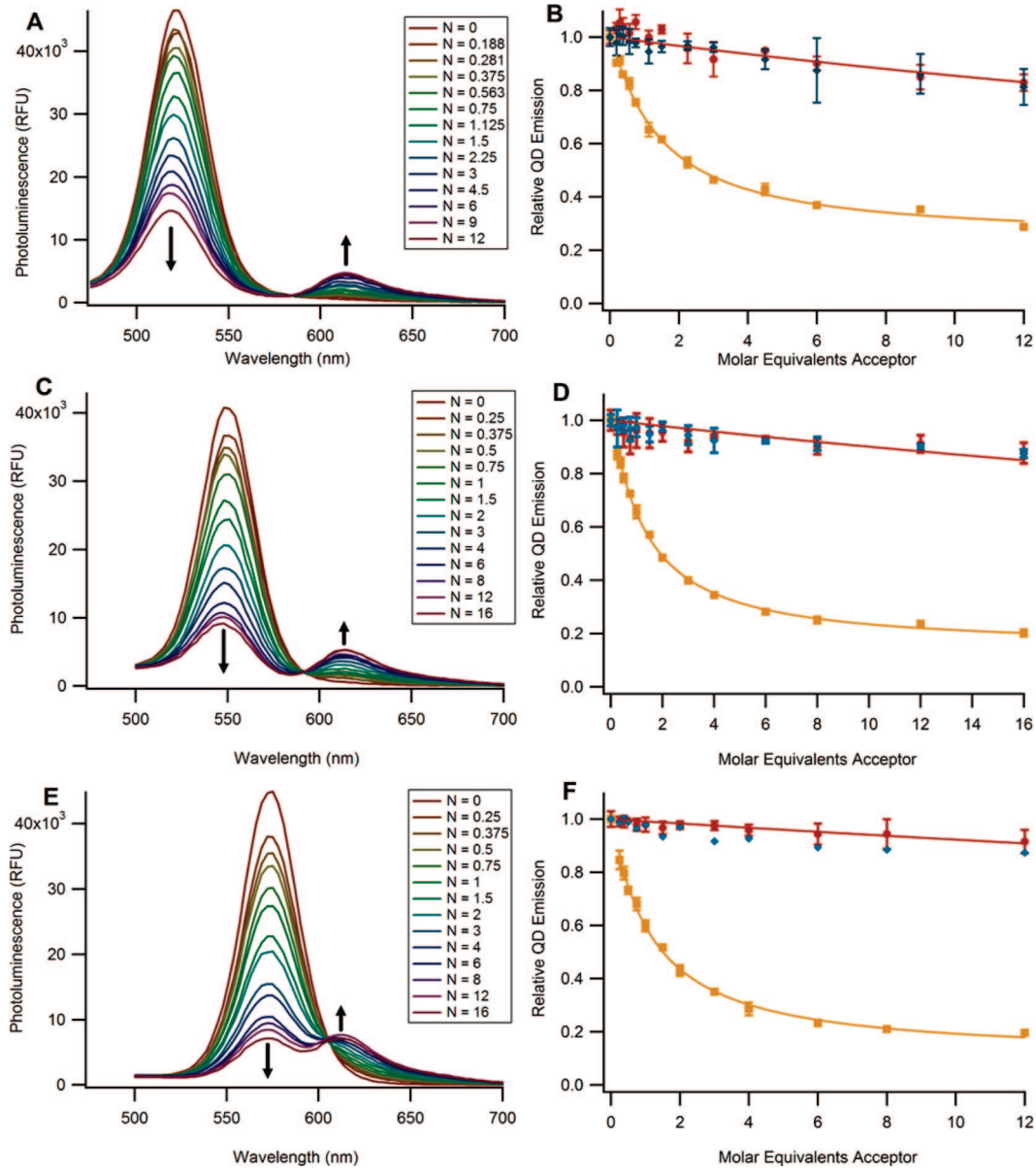

Figure 4. FRET results using the fluorescent protein mCherry as acceptor and a QD donor. (A, C, and E) Spectra of QD520 + His6-mCherry, QD540 + His6-mCherry, and QD560 + His6-mCherry, respectively. *N* is the average number of fluorescent proteins per QD. (B, D, and F) Relative area under the QD emission peak of background-subtracted spectra. The non-his-tagged FP control is represented as a circle (●), the His10-only (no fluorescent protein) control is a diamond (♦), and the His6-FP is represented by a square (■). Data are represented as a mean ± standard deviation of $n = 3$.

quenching of the QDs (see Supporting Information). Note that this nominal K_D is not the acceptor concentration at which there is 50% FPs binding to QDs, since the fluorescent quenching may not be linearly related to the number of acceptors bound.[18,20] The FRET efficiencies at each specific QD:FP ratio (E) were calculated using the equation[20]

$$E = 1 - \frac{F_{DA}}{F_D} \tag{4}$$

The FRET efficiency with 1:1 QD:FP ratios, the maximum FRET efficiency, and the dissociation constant for each FRET pair are listed in Table 2.

As shown in Figures 3 and 4, all six of the QD-FP FRET pairs demonstrated a significant level of energy transfer with 26−50% QD quenching at a 1:1 QD:FP ratio and up to 90% quenching at higher QD:FP ratios. While the increased molar extinction coefficient of tdTomato did make it a more effective quencher than the monomeric mOrange and mCherry, the difference was not dramatic enough for one to choose tdTomato over mCherry when probe size is a concern. The non-his-tagged and His10 controls produced minimal quenching of the EviTags, demonstrating that the effect was neither due to contact quenching nor due to the presence of freely dispersed fluorescent protein, but rather the presence of both the polyhistidine and the fluorescent protein was necessary for effective quenching. As seen in Table 2, the binding of the his-tagged proteins to the EviTags had a nominal K_D between 40 and 100 nM, which is in the range of dissociation constants described for antigen−antibody binding.[29] This binding strength indicates that the his-tag conjugation to the commercially available EviTags should

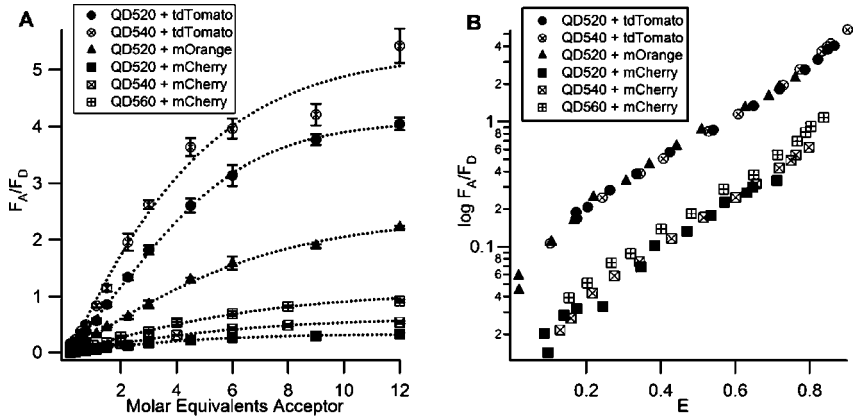

Figure 5. Ratiometric analysis of FRET assays. (A) The acceptor emission/donor emission as a function of acceptor concentration. Data are represented as a mean ± standard deviation of $n = 3$ and vary greatly depending on the brightness of the fluorescent protein. (B) The log of the acceptor emission/donor emission as a function of FRET efficiency. Each point is the mean of data taken in triplicate.

be sufficient for use in *in vitro* assays. FPs containing a His10 N-terminal insertion were also tested in the FRET assay with the hypothesis that the longer polyhistidine-tag may increase the binding affinity, as is seen in IMAC.[30] No significant difference between the nominal K_D values of the His6-FPs and His10-FPs was observed (data not shown), however, which is consistent with other reports in the literature.[22]

Using the FRET efficiencies determined for each QD:FP ratio and the Förster distance calculated for each FRET pair, R, the distance between the donor and the acceptor was estimated using an equation that takes into account the binding of multiple acceptor FPs to each donor QD. The equation used for the FRET efficiency as a function of n, the average number of acceptors attached to the donor, is given by[18,20]

$$E(n) = \frac{nR_0^6}{nR_0^6 + R^6} \tag{5}$$

For any given ratio of donors to acceptors (or average number of acceptors per donor), the specific number of acceptors, k, attached to the donors is described by Poisson's distribution[31]

$$p(k, n) = \frac{n^k e^{-n}}{k!} \tag{6}$$

The efficiency of the FRET interaction can be more accurately calculated for each donor−acceptor ratio using a weighted distribution of efficiencies, taking into account the effect of the Poisson distribution[14,32]

$$E(n) = \sum_n p(k, n)E(k) = \sum_{k=1}^{\infty} \frac{n^k e^{-n}}{k!} \frac{kR_0^6}{(kR_0^6 + R^6)} \tag{7}$$

We used Mathematica (v.6.0.1, Wolfram Research, Inc., Champaign, IL) to solve this equation for R for each value of n for each FRET pair; the average and standard deviation for R for each FRET pair is presented in Table 2. All of the donor−acceptor pairs displayed a separation distance of 5−6 nm. While compared to the relatively small differences in the QD sizes the standard deviations on these values are too large to show correlations between the QD core−shell radius and the distance between the donor and acceptor, all of the values are consistent with the fluorescent protein binding to the QD core−shell surface.

To highlight differences in the various FP acceptors, the FRET data were also analyzed using a ratiometric method, where the emission of the acceptor was divided by the emission from the donor and plotted in Figure 5A as a function of the molar equivalent of the acceptor. While all three of the fluorescent proteins were shown to be effective quenchers of the QD emission, this ratiometric analysis demonstrates the contrast between the emissions of the three proteins. For example, the three FRET pairs containing mCherry showed only a small increase in F_A/F_D due to the low quantum yield of the FP, while the FRET pairs containing tdTomato demonstrated a dramatic increase because of the exceptional brightness of tdTomato. mOrange fell between the two in the increase of F_A/F_D as it possesses a quantum yield as high as that of tdTomato, but like mCherry, it has only half the molar extinction coefficient compared with tdTomato due to its monomeric form. The distinction between different FPs based on their emission properties was further demonstrated in Figure 5B by plotting the log of F_A/F_D as a function of the FRET efficiency. When the effect of the absorption characteristics of the FPs is eliminated, the six QD-FP pairs split into two groups: those containing the more efficient emitters mOrange or tdTomato and those containing mCherry. Note that tdTomato and mOrange converged almost completely because both have quantum yields of 0.69 (Table 1). This difference between the FPs can be exploited in probe design: using the quencher-like mCherry allows one to neglect the acceptor emission for a more straightforward data analysis, whereas tdTomato is preferred when the ratiometric method could be used in data analysis to extend the range of an assay or to minimize the effects of well-to-well variation.

In summary, this study characterized six FP-QD FRET pairs and demonstrated that mOrange, mCherry, and tdTomato are efficient FRET acceptors when paired with a quantum dot donor. It also demonstrated that polyhistidine coordination to the QD core−shell surface can be utilized as a straightforward and effective means of conjugating proteins to commercially available QDs. These findings have signifi-

cant implications for the development of versatile and easily accessible QD-based FRET probes for biomedical applications, including ultrasensitive *in vitro* assays for measuring enzymatic activity using an enzyme-cleavable sequence between the QD and FP that form a FRET pair.

Acknowledgment. The authors acknowledge laboratory support from David Sotto and Marc Seaman as well as helpful discussions with Dr. Philip Santangelo and Jeffery Stirman. This work was supported by the National Heart Lung and Blood Institute of the NIH as a Program of Excellence in Nanotechnology (HL80711), by the National Cancer Institute of the NIH as a Center of Cancer Nanotechnology Excellence (CA119338), and by DoE (DE-FG02-04ER63785). Financial support for A.M.D. was also provided by a National Defense Science and Engineering Graduate (NDSEG) Fellowship (2004−2007).

Supporting Information Available: Details of the plasmid mutagenesis, protein expression and purification, spectra of the direct excitation of the His6-FPs in the FRET assays, details of the Stern−Volmer analysis performed on the non-his-tagged FP FRET assay data, a discussion of the modifications made to the conventional Hill equation, and all of the fitted coefficients from the Hill equation and the Stern−Volmer equation. This material is available free of charge via the Internet at http://pubs.acs.org.

References

(1) Chan, W. C.; Nie, S. Quantum dot bioconjugates for ultrasensitive nonisotopic detection. *Science* **1998**, *281* (5385), 2016–2018.
(2) Bruchez, M.; Moronne, M.; Gin, P.; Weiss, S.; Alivisatos, A. P. Semiconductor nanocrystals as fluorescent biological labels. *Science* **1998**, *281* (5385), 2013–2016.
(3) Voura, E. B.; Jaiswal, J. K.; Mattoussi, H.; Simon, S. M. Tracking metastatic tumor cell extravasation with quantum dot nanocrystals and fluorescence emission-scanning microscopy. *Nat. Med.* **2004**, *10* (9), 993–998.
(4) Garon, E. B.; Marcu, L.; Luong, Q.; Tcherniantchouk, O.; Crooks, G. M.; Koeffler, H. P. Quantum dot labeling and tracking of human leukemic, bone marrow and cord blood cells. *Leuk. Res.* **2007**, *31* (5), 643–651.
(5) Hama, Y.; Koyama, Y.; Urano, Y.; Choyke, P. L.; Kobayashi, H. Simultaneous two-color spectral fluorescence lymphangiography with near infrared quantum dots to map two lymphatic flows from the breast and the upper extremity. *Breast Cancer Res. Treat.* **2007**, *103* (1), 23–28.
(6) Gao, X.; Cui, Y.; Levenson, R. M.; Chung, L. W.; Nie, S. In vivo cancer targeting and imaging with semiconductor quantum dots. *Nat. Biotechnol.* **2004**, *22* (8), 969–976.
(7) Chattopadhyay, P. K.; Price, D. A.; Harper, T. F.; Betts, M. R.; Yu, J.; Gostick, E.; Perfetto, S. P.; Goepfert, P.; Koup, R. A.; De Rosa, S. C.; Bruchez, M. P.; Roederer, M. Quantum dot semiconductor nanocrystals for immunophenotyping by polychromatic flow cytometry. *Nat. Med.* **2006**, *12* (8), 972–977.
(8) Howarth, M.; Takao, K.; Hayashi, Y.; Ting, A. Y. Targeting quantum dots to surface proteins in living cells with biotin ligase. *Proc. Natl. Acad. Sci. U.S.A.* **2005**, *102* (21), 7583–7588.
(9) Bonasio, R.; Carman, C. V.; Kim, E.; Sage, P. T.; Love, K. R.; Mempel, T. R.; Springer, T. A.; von Andrian, U. H. Specific and covalent labeling of a membrane protein with organic fluorochromes and quantum dots. *Proc. Natl. Acad. Sci. U.S.A.* **2007**, *104* (37), 14753–14758.
(10) Chang, E.; Miller, J. S.; Sun, J.; Yu, W. W.; Colvin, V. L.; Drezek, R.; West, J. L. Protease-activated quantum dot probes. *Biochem. Biophys. Res. Commun.* **2005**, *334* (4), 1317–1321.
(11) Xu, C.; Xing, B.; Rao, J. A self-assembled quantum dot probe for detecting beta-lactamase activity. *Biochem. Biophys. Res. Commun.* **2006**, *344* (3), 931–935.
(12) Clapp, A. R.; Medintz, I. L.; Uyeda, H. T.; Fisher, B. R.; Goldman, E. R.; Bawendi, M. G.; Mattoussi, H. Quantum Dot-Based Multiplexed Fluorescence Resonance Energy Transfer. *J. Am. Chem. Soc.* **2005**, *127* (51), 18212–18221.
(13) Yao, H.; Zhang, Y.; Xiao, F.; Xia, Z.; Rao, J. Quantum dot/bioluminescence resonance energy transfer based highly sensitive detection of proteases. *Angew. Chem., Int. Ed.* **2007**, *46* (23), 4346–4349.
(14) Medintz, I. L.; Clapp, A. R.; Brunel, F. M.; Tiefenbrunn, T.; Uyeda, H. T.; Chang, E. L.; Deschamps, J. R.; Dawson, P. E.; Mattoussi, H. Proteolytic activity monitored by fluorescence resonance energy transfer through quantum-dot-peptide conjugates. *Nat. Mater.* **2006**, *5* (7), 581–589.
(15) Sapsford, K. E.; Pons, T.; Medintz, I. L.; Mattoussi, H. Biosensing with luminescent semiconductor quantum dots. *Sensors* **2006**, *6* (8), 925–953.
(16) Qu, L.; Peng, X. Control of photoluminescence properties of CdSe nanocrystals in growth. *J. Am. Chem. Soc.* **2002**, *124* (9), 2049–2055.
(17) Striolo, A.; Ward, J.; Prausnitz, J. M.; Parak, W. J.; Zanchet, D.; Gerion, D.; Milliron, D.; Alivisatos, A. P. Molecular weight, osmotic second virial coefficient, and extinction coefficient of colloidal CdSe nanocrystals. *J. Phys. Chem. B* **2002**, *106* (21), 5500–5505.
(18) Medintz, I. L.; Clapp, A. R.; Mattoussi, H.; Goldman, E. R.; Fisher, B.; Mauro, J. M. Self-assembled nanoscale biosensors based on quantum dot FRET donors. *Nat. Mater.* **2003**, *2* (9), 630–638.
(19) Chan, W. C. W.; Maxwell, D. J.; Gao, X. H.; Bailey, R. E.; Han, M. Y.; Nie, S. M. Luminescent quantum dots for multiplexed biological detection and imaging. *Curr. Opin. Biotechnol.* **2002**, *13* (1), 40–46.
(20) Lakowicz, J. R., *Principles of fluorescence spectroscopy*, 3rd ed.; Springer: New York, 2006.
(21) Clapp, A. R.; Medintz, I. L.; Mattoussi, H. Forster resonance energy transfer investigations using quantum-dot fluorophores. *ChemPhysChem* **2006**, *7* (1), 47–57.
(22) Sapsford, K. E.; Pons, T.; Medintz, I. L.; Higashiya, S.; Brunel, F. M.; Dawson, P. E.; Mattoussi, H. Kinetics of Metal-Affinity Driven Self-Assembly between Proteins or Peptides and CdSe-ZnS Quantum Dots. *J. Phys. Chem. C* **2007**, *111* (31), 11528–11538.
(23) Susumu, K.; Uyeda, H. T.; Medintz, I. L.; Pons, T.; Delehanty, J. B.; Mattoussi, H. Enhancing the stability and biological functionalities of quantum dots via compact multifunctional ligands. *J. Am. Chem. Soc.* **2007**, *129* (45), 13987–13996.
(24) Shaner, N. C.; Campbell, R. E.; Steinbach, P. A.; Giepmans, B. N.; Palmer, A. E.; Tsien, R. Y. Improved monomeric red, orange and yellow fluorescent proteins derived from Discosoma sp. red fluorescent protein. *Nat. Biotechnol.* **2004**, *22* (12), 1567–1572.
(25) Shaner, N. C.; Steinbach, P. A.; Tsien, R. Y. A guide to choosing fluorescent proteins. *Nat. Methods* **2005**, *2* (12), 905–909.
(26) Moreland, J. L.; Gramada, A.; Buzko, O. V.; Zhang, Q.; Bourne, P. E. The Molecular Biology Toolkit (MBT): a modular platform for developing molecular visualization applications. *BMC Bioinf.* **2005**, *6*, 21.
(27) Hink, M. A.; Visser, N. V.; Borst, J. W.; van Hoek, A.; Visser, A. J. W. G. Practical use of corrected fluorescence excitation and emission spectra of fluorescent proteins in Forster resonance energy transfer (FRET) studies. *J. Fluoresc.* **2003**, *13* (2), 185–188.
(28) Guignet, E. G.; Hovius, R.; Vogel, H. Reversible site-selective labeling of membrane proteins in live cells. *Nat. Biotechnol.* **2004**, *22* (4), 440–444.
(29) Harlow, E.; Lane, D., *Antibodies: a laboratory manual*; Cold Spring Harbor Laboratory: Cold Spring Harbor, NY, 1988.
(30) Hoffmann, A.; Roeder, R. G. Purification of his-tagged proteins in non-denaturing conditions suggests a convenient method for protein interaction studies. *Nucleic Acids Res.* **1991**, *19* (22), 6337–6338.
(31) Pons, T.; Medintz, I. L.; Wang, X.; English, D. S.; Mattoussi, H. Solution-phase single quantum dot fluorescence resonance energy transfer. *J. Am. Chem. Soc.* **2006**, *128* (47), 15324–15331.
(32) Medintz, I. L.; Berti, L.; Pons, T.; Grimes, A. F.; English, D. S.; Alessandrini, A.; Facci, P.; Mattoussi, H. A reactive peptidic linker for self-assembling hybrid quantum dot-DNA bioconjugates. *Nano Lett.* **2007**, *7* (6), 1741–1748.

NL080358+